ELSEVIER

Journal of Molecular Liquids 125 (2006) 37 – 44

journal of MOLECULAR LIQUIDS

www.elsevier.com/locate/molliq

Modeling phase equilibria and speciation in mixed-solvent electrolyte systems: II. Liquid–liquid equilibria and properties of associating electrolyte solutions ☆

P. Wang *, A. Anderko, R.D. Springer, R.D. Young

OLI Systems, Inc., 108 American Road, Morris Plains, NJ 07950, U.S.A.

Available online 4 January 2006

Abstract

A comprehensive mixed-solvent electrolyte model has been extended to calculate liquid–liquid equilibria in water–organic salt systems. Also, it has been applied to calculate phase equilibria and speciation in strongly associating systems such as sulfuric acid/oleum (H_2SO_4+SO_3+H_2O) in the entire concentration range. The model combines an excess Gibbs energy model with detailed speciation calculations. The excess Gibbs energy model consists of a long-range interaction contribution represented by the Pitzer–Debye–Hückel expression, a short-range term expressed by the UNIQUAC model and a middle-range term of a second-virial-coefficient type for specific ionic interactions. The model accurately represents the thermodynamic behavior of systems ranging from infinite dilution in water to pure acids and beyond, e.g. in mixtures of H_2SO_4 and SO_3. In particular, the model has been shown to predict speciation that is consistent with spectroscopic measurements for the H_2SO_4+H_2O system. In addition, vapor–liquid and liquid–liquid equilibria can be accurately reproduced in mixtures that show complex phase behavior.

Keywords: Electrolytes; Liquid–liquid equilibria; Speciation; Vapor–liquid equilibria

1. Introduction

Accurate representation of chemical and phase equilibria in mixed-solvent electrolyte systems is of great importance in fundamental research and for the design of numerous chemical processes including extractive distillation, solution crystallization, desalination, and wastewater treatment. An important feature of electrolyte systems is the fact that phase equilibria and other thermodynamic properties are inherently affected by speciation equilibria, which may be due to ion-pairing, acid–base reactions, and complexation. Modeling of relationships between chemical speciation and phase equilibria in mixed-solvent electrolyte systems can provide insight into structural phenomena such as solvation of ions and the change in ionic interactions with changing solvent environment. Recently, a general, speciation-based thermodynamic model has been developed for mixed-solvent electrolyte solutions [1]. This model was shown to reproduce simultaneously vapor–liquid equilibria, solid–liquid equilibria, speciation, caloric and volumetric properties of electrolytes in organic or mixed (organic–water) solvents. The model is valid for salts from infinite dilution to the fused salt limit and for various completely miscible inorganic systems (such as acid–water mixtures) over a full concentration range. Also, the model is capable of representing phase equilibria in multicomponent inorganic systems containing two salts and water or a salt, an acid and water [2]. Complex phase behavior such as formation of multiple hydrated salts, double salts, or the presence of eutectic points has been accurately represented.

In this study, we apply the model to the computation of liquid–liquid equilibria in mixed-solvent electrolyte systems and examine its capability of reproducing simultaneously vapor–liquid and liquid–liquid equilibria for systems that show complex phase behavior. In particular, the effect of electrolytes on LLE is studied for several organic+water mixtures. In addition, a comprehensive analysis is performed to examine systems that are conventionally regarded as "strong acids" but show significant speciation effects. We focus on the H_2SO_4+H_2O+SO_3 system in a very wide range of concentra-

☆ Paper presented at the 18th IUPAC International Conference on Chemical Thermodynamics, August 17–21, 2004, Beijing, China.

* Corresponding author. Fax: +1 973 539 5922.
E-mail address: pwang@olisystems.com (P. Wang).

0167-7322/$ - see front matter © 2005 Elsevier B.V. All rights reserved.
doi:10.1016/j.molliq.2005.11.030

tions, which covers not only the H_2SO_4+H_2O binary but also extends to the oleum region (i.e., mixtures of H_2SO_4+SO_3). Speciation effects in this system are examined and compared with experimental results from spectroscopic measurements.

2. Thermodynamic framework

The thermodynamic framework has been established [1] by combining an excess Gibbs energy model for mixed-solvent electrolyte systems with a comprehensive treatment of chemical equilibria. In this framework, the excess Gibbs energy is expressed as

$$\frac{G^{ex}}{RT} = \frac{G^{ex}_{LR}}{RT} + \frac{G^{ex}_{MR}}{RT} + \frac{G^{ex}_{SR}}{RT} \tag{1}$$

where G^{ex}_{LR} represents the contribution of long-range electrostatic interactions, G^{ex}_{SR} is the short-range contribution resulting from intermolecular interactions, and an additional (middle-range) term G^{ex}_{MR} represents primarily ionic interactions (i.e., ion/ion and ion/molecule) that are not accounted for by the long-range term. The rationale and derivation of Eq. (1) was discussed in detail by Wang et al. [1] and, therefore, only the basic features of the model are summarized here.

The long-range interaction contribution is calculated from the Pitzer–Debye–Hückel formula [3, 4] expressed in terms of mole fractions and symmetrically normalized, i.e.,

$$\frac{G^{ex}_{DH}}{RT} = -\left(\sum_i n_i\right)\frac{4A_xI_x}{\rho}\ln\left(\frac{1+\rho I_x^{1/2}}{\sum_i x_i\left[1+\rho\left(I^0_{x,i}\right)^{1/2}\right]}\right) \tag{2}$$

where the sum is over all species, I_x is the mole fraction-based ionic strength, $I^0_{x,i}$ represents the ionic strength when the system composition reduces to a pure component i, i.e., $I^0_{x,i}=1/2z_i^2$; ρ is related to the hard-core collision diameter ($\rho=14.0$) and the A_x parameter is given by

$$A_x = \frac{1}{3}(2\pi N_A d_s)^{1/2}\left(\frac{e^2}{4\pi\varepsilon_0\varepsilon_s k_B T}\right)^{3/2} \tag{3}$$

where d_s and ε_s are the molar density and the dielectric constant of the solvent, respectively. The dielectric constant is calculated from an expression developed previously for mixed solvents [5].

For the short-range interaction contribution, the UNIQUAC equation [6] is used. The middle-range interaction contribution is calculated from an ionic strength-dependent, symmetrical second-virial-coefficient-type expression [1]:

$$\frac{G^{ex}_{MR}}{RT} = -\left(\sum_i n_i\right)\sum_i\sum_j x_ix_jB_{ij}(I_x) \tag{4}$$

where $B_{ij}(I_x)=B_{ji}(I_x)$, $B_{ii}=B_{jj}=0$ and the ionic strength dependence of B_{ij} is given by

$$B_{ij}(I_x) = b_{ij} + c_{ij}\exp\left(-\sqrt{I_x+a_1}\right) \tag{5}$$

where b_{ij} and c_{ij} are adjustable parameters and a_1 is set equal to 0.01. In general, the parameters b_{ij} and c_{ij} are calculated as functions of temperature as

$$b_{ij} = b_{0,ij} + b_{1,ij}T + b_{2,ij}/T \tag{6}$$

$$c_{ij} = c_{0,ij} + c_{1,ij}T + c_{2,ij}/T. \tag{7}$$

In practice, the middle-range parameters are used to represent ion–ion and ion–neutral molecule interaction. The short-range parameters are used primarily for interaction between neutral molecules.

Speciation effects due to the formation of ion pairs and complexes are explicitly taken into account using chemical equilibria. Chemical equilibrium calculations require the standard-state chemical potential, μ^0_i, for all species together with activity coefficients. The standard-state chemical potentials for aqueous species are calculated as functions of temperature and pressure using the Helgeson–Kirkham–Flowers equation of state [7]. The parameters of this model are available for a large number of aqueous species including ions, associated ion pairs, and neutral species [8–11]. It should be noted that standard-state properties calculated from the model of Helgeson et al. are based on the infinite-dilution reference state and on the molality concentration scale. To make the speciation calculations consistent when the standard-state properties are combined with the mole fraction-based and symmetrically normalized activity coefficients, the following conversions are performed: (1) the activity coefficients calculated from Eq. (1) are converted to those based on the unsymmetrical reference state, i.e. at infinite dilution in water, as described by Wang et al. [1], and (2) the molality-based standard-state chemical potentials are converted to a corresponding mole fraction-based quantity.

For speciation calculations in organic or mixed-solvent electrolyte solutions, the chemical potential of the species is modeled by combining aqueous standard-state properties with accurately predicted Gibbs energies of transfer. This is achieved by constraining the activity coefficient model parameters so that the Gibbs energy of transfer of ions from water to a non-aqueous solvent can be reproduced [1]. The general expression that relates the Gibbs energy of transfer to the activity coefficients is as follows:

$$\Delta_{tr}G^0_i(\mathrm{R}\rightarrow\mathrm{S})_m = RT\ln\frac{\gamma_i^{*,\mathrm{S}}\cdot M_S}{\gamma_i^{*,\mathrm{R}}\cdot M_R} \tag{8}$$

where M_x (X=S or R) are the molecular weights of solvent X and $\gamma_i^{*,X}$ is the mole fraction-based unsymmetrical activity coefficient of ion i in solvent X.

3. Liquid–liquid equilibria in mixed-solvent electrolyte systems

Earlier studies on modeling liquid–liquid equilibria in mixed-solvent electrolyte systems have been reported by Zuo et al. [12], Zerres and Prausnitz [13], and Liu and Watanasiri [14]. When two liquid phases, α and β, are in equilibrium, the

chemical potentials for each component i are equal in the two coexisting phases, i.e.,

$$\mu_i^{\alpha} = \mu_i^{\beta}. \tag{9}$$

In electrolyte solutions, although cations and anions appear as separate species, only the chemical potential of an electrically neutral salt is experimentally accessible due to the electroneutrality condition. Thus, in a system containing a single cation C and a single anion A, at a given temperature and pressure, the chemical potential of the electrolyte, $C_{v_c}A_{v_a}$, can be expressed as

$$\mu_{C_{v_c}A_{v_a}} = v_c\mu_C + v_a\mu_A. \tag{10}$$

Substituting Eq. (11), which defines the chemical potential,

$$\mu_i = \mu_i^0 + RT\ln(\gamma_i x_i) \tag{11}$$

into Eq. (10), we obtain

$$\mu_{C_{v_c}A_{v_a}} = \left(v_c\mu_C^0 + v_a\mu_A^0\right) + vRT\ln(\gamma_{\pm}x_{\pm}) \tag{12}$$

where $v = v_c + v_a$, and

$$\gamma_{\pm} = \left(\gamma_C^{v_c}\gamma_A^{v_a}\right)^{1/v} \tag{13a}$$

$$x_{\pm} = \left(x_C^{v_c}x_A^{v_a}\right)^{1/v}. \tag{13b}$$

The LLE criterion for the electrolyte can be derived by substituting Eq. (12) into Eq. (9):

$$(\gamma_{\pm}x_{\pm})^{\alpha} = (\gamma_{\pm}x_{\pm})^{\beta}. \tag{14}$$

When the system contains multiple ions, this constraint must be applied for an independent set of cation–anion pairs. In the case of neutral species j, the equilibrium condition reduces to

$$\left(\gamma_j x_j\right)^{\alpha} = \left(\gamma_j x_j\right)^{\beta}. \tag{15}$$

In the computation of liquid–liquid equilibria, ionic reaction equilibria are included for both coexisting liquid phases and the excess Gibbs energy model (Eq. (1)) is used for calculating activity coefficients in both phases. One of the advantages of using a symmetrical reference state in the activity coefficient model is that it ensures the consistency of LLE calculations.

It should be noted that a complete thermodynamic treatment of liquid–liquid equilibria in multicomponent electrolyte systems would necessitate taking into account the electrostatic contact potential between the two coexisting phases. As discussed by Pratt [15], electrostatic surface potentials can be quantitatively introduced on the basis of the knowledge of either single-ion activities or high-resolution structural information on interfacial charge densities. Specifically, the computation of the contact potential would require solving the equality of chemical potentials redefined as $\mu_i = \mu_i^0 + \mathrm{RTln}a_i^{\mathrm{chemical}} + z_i F\Phi$, where Φ is the electrostatic potential, for individual ions in two coexisting phases. Then, the difference in the electrostatic potential in both phases would yield the contact potential. As discussed by Haynes et al. [16,17], the knowledge of the interfacial potential is not required for the determination of equilibrium compositions, but is useful for understanding the structure and intermolecular forces acting at the interface.

The model described in this study, being of a practically oriented, engineering nature, is not predicated on the assumption that information on single-ion activities is available. Instead, the model is designed to simulate the partitioning of salts and other components between two phases. Thus, the equilibrium is found by equating the chemical potentials of neutral cation–anion pairs in both phases as represented by Eq. (10). In such a procedure, the terms containing Φ cancel in the calculations. This procedure is applicable to multicomponent systems provided that a linearly independent set of neutral cation–anion combinations is defined. Such combinations typically correspond to actual salts. It can be easily shown that once the equality of chemical potentials is satisfied for a linearly independent set of cation–anion combinations, it is also satisfied for any other combination.

4. Results

Extensive literature data have been used to validate the model for various classes of mixtures. Sample results have been previously reported [1,2] for vapor–liquid equilibria, solid–liquid equilibria, osmotic and activity coefficients, densities, heats of mixing and dilution, heat capacities, and selected speciation-related data (pH, acid dissociation constants, etc.) for a number of electrolyte systems. In this study, we first examine the simultaneous representation of vapor–liquid and liquid–liquid equilibria for systems that show complex phase behavior. Then, we focus on modeling the effect of electrolytes on liquid–liquid equilibria in mixed-solvent electrolyte systems. Finally, we perform a comprehensive study of the system sulfuric acid/oleum. The selection of these systems is largely based on their practical importance, strong speciation effects, and the availability of comprehensive experimental data.

4.1. Simultaneous representation of VLE and LLE

When VLE and LLE data are simultaneously represented using a single set of UNIQUAC parameters, it is well known that there is a notable loss of accuracy in the representation of experimental data [18]. Liquid–liquid equilibria are much more sensitive to binary parameters than vapor–liquid equilibria [19] and simultaneously correlation of VLE and LLE becomes especially challenging for systems exhibiting complex phase behavior. For example, in the phenol+water system, the mixture separates into two liquid phases with a critical solution temperature of ~67 °C located at x (phenol) ≈ 0.10. Thus, the liquid–liquid equilibrium is represented by a highly unsymmetrical binodal curve in a T–x diagram. At the same time, the system shows azeotropic behavior with an atmospheric-pressure azeotropic point located at x (phenol) ≈ 0.02 and T ≈ 99.6 °C. When UNIQUAC is used alone, simultaneous representation of VLE and LLE cannot be achieved. To solve this problem, we utilize the middle-range term (Eq. (4)) in addition to using the classical UNIQUAC equation for non-

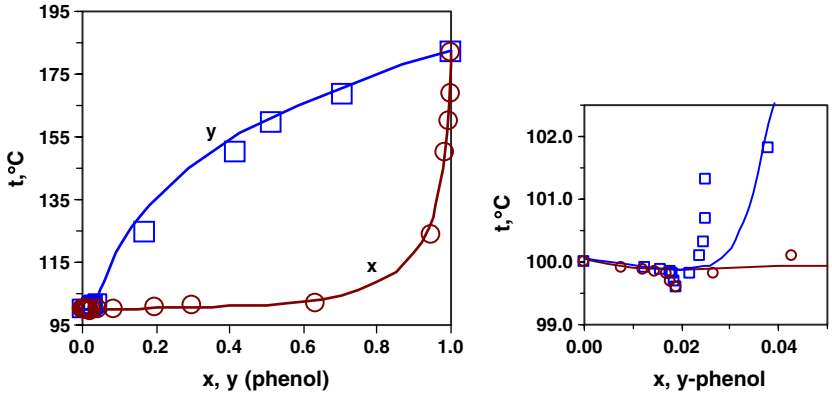

Fig. 1. Calculated and experimental VLE results for the phenol+H_2O system at 1 atm. The symbols represent the data of Brusset and Gaynes [20].

electrolyte mixtures. This greatly improves the fit without compromising the accuracy of either VLE or LLE calculations. The results of simultaneously correlating VLE and LLE data in the phenol+water system are shown in Figs. 1 and 2. The parameters obtained for this system are listed in Table 1.

4.2. Effect of electrolytes on LLE

Salt effect on liquid–liquid equilibria is of importance for many applications such as separation of organic components from aqueous solutions or precipitation of proteins. The solubility of an organic solute in aqueous solutions often decreases upon the addition of an electrolyte. This phenomenon is commonly referred to as "salting-out". Experimental data on the effect of salts on LLE are dominated by solubilities of organic solutes in aqueous solutions. In contrast, data on the effect of salt on the solubility of water in organic solvents are less common. In this study, we have examined several systems for which the available LLE data are relatively complete and we have developed model parameters for predicting the changes of solubility in both the aqueous and organic phases as the electrolyte concentration increases. Table 2 summarizes the parameters obtained by simultaneously fitting VLE and LLE data for the binary system benzene+H_2O and LLE data for the NaCl+benzene+H_2O ternary. Further, Fig. 3 shows the results obtained for the solubilities of benzene in aqueous solutions of NaCl and $(NH_4)_2SO_4$ as a function of the electrolyte concentration. Solubilities of benzene and cyclohexane in aqueous solutions of NaCl are shown in Fig. 4 with experimental and calculated results plotted as a function of NaCl concentration. Solubility of water in an organic solvent is illustrated in Fig. 5 for the system NaCl+benzene+water. All these figures show that the model is capable of accurately representing LLE in mixed-solvent electrolyte systems.

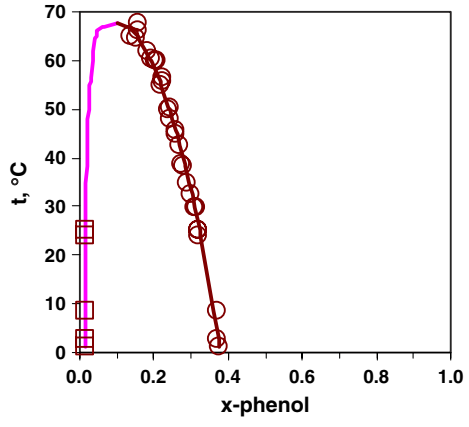

Fig. 2. Calculated and experimental LLE results for the phenol+H_2O system. The symbols show the data of Campbell [21], Campbell and Campbell [22], Prutton et al. [23], Lyzlova and Susarev [24], and Schreinemakers [25].

4.3. Sulfuric acid/oleum system

This system is of considerable practical interest because both sulfuric acid and oleum (the mixture of SO_3+H_2SO_4) are among the most important primary products in the chemical industry. Therefore, an accurate model for this system is highly desirable. Due to significant ion association effects that depend strongly on acid concentration, thermodynamic modeling of this system is unusually difficult. Preliminary investigation of this system was carried out in a previous paper [1] in the concentration range of $x_{H_2SO_4}$ from 0 to 1. Although the thermodynamic properties (VLE, ΔH_{dil}, C_p, density) were accurately reproduced in that study, speciation results (i.e. the change in acid dissociation with concentration) agreed with experimental Raman and NMR measurements [33–35] only at low concentrations of sulfuric acid. At higher concentrations, the calculated results, although qualitatively consistent with the spectroscopic data, showed significantly smaller concentrations of undissociated $H_2SO_4^0$. Thus, it was necessary to improve the model because accurate prediction of speciation is highly

Table 1
Model parameters for the system phenol+water

UNIQUAC parameters, a_{ij} and a_{ji}^*	Mid-range parameters, b_{ij} and c_{ij}^{**}
a_0 (phenol, H_2O)=4443.384	b_0 (H_2O, phenol)=2.566712
a_1 (phenol, H_2O)=−27.92888	b_1 (H_2O, phenol)=−0.006353166
a_2 (phenol, H_2O)=0.016816089	b_2 (H_2O, phenol)=−321.601
a_0 (H_2O, phenol)=−18365.45	c_0 (H_2O, phenol)=2.908486
a_1 (H_2O, phenol)=123.6591	c_1 (H_2O, phenol)=−0.005570462
a_2 (H_2O, phenol)=−0.1517114	c_2 (H_2O, phenol)=−314.2246

*$a_{ij}=a_0+a_1T+a_2T^2$; units for a_{ij} and a_{ji} are J mol^{-1};
**b_{ij} and c_{ij} are defined in Eqs. (6) and (7), they are dimensionless.

Table 2
Model parameters for the system NaCl+benzene+H_2O*

UNIQUAC parameters, a_{ij} and a_{ji}	Mid-range parameters, b_{ij}^{**}
a_0(benzene, H_2O)=9637.066	b_0(benzene, Na^+)=−13.43095
a_1(benzene, H_2O)=9.043689	b_1(benzene, Na^+)=0.00562622
a_2(benzene, H_2O)=−0.057217179	b_2(benzene, Na^+)=0
a_0(H_2O, benzene)=−2002.344	b_0(benzene, Cl^-)=−9.75623
a_1(H_2O, benzene)=27.43204	b_1(benzene, Cl^-)=−0.002448221
a_2(H_2O, benzene)=−0.035465071	b_2(benzene, Cl^-)=0

*See footnote in Table 1 for units in the parameters;
**All c_{ij} are set to be zero.

desirable especially for modeling transport phenomena and electrochemical processes.

A literature search has revealed the availability of extensive experimental data for this system. The data include not only phase equilibria, activities, enthalpies, heat capacities, and densities over wide ranges of temperature, pressure and concentration, but also speciation as a function of acid concentration. These data provide an excellent foundation for a comprehensive treatment of this system and for testing the model's capability of reproducing both thermodynamic properties and speciation in the entire concentration range from 0% to 100% H_2SO_4 (H_2SO_4+H_2O) and beyond, i.e. from pure H_2SO_4 to 100% SO_3 (H_2SO_4+SO_3).

In the present work, the thermodynamics of the H_2SO_4+SO_3+H_2O system has been treated using two alternative approaches to speciation calculations. In the first approach, the chemistry of the system is determined by conventional dissociation reactions according to which sulfuric acid dissociates to form HSO_4^-, SO_4^{-2} and H^+. This treatment is similar to that discussed in the previous paper [1], except for the fact that a substantially extended concentration range (i.e., H_2SO_4+SO_3) is covered. Also, we apply the model to a much wider range of temperatures, i.e., up to 500 °C. Extension of the model to such high temperatures necessitates a modification of the treatment of standard-state properties above 300 °C, which is described in the Appendix.

This classical approach leads to a reasonable agreement with experimental phase equilibria, activities, and other

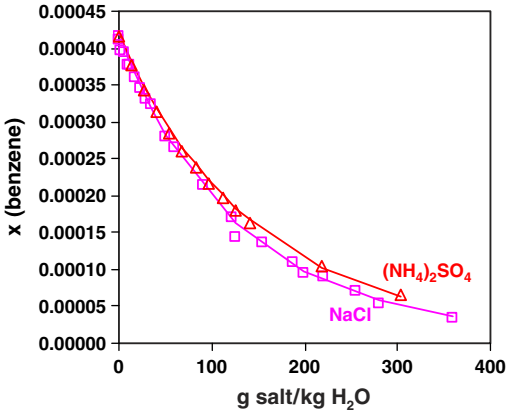

Fig. 3. Calculated and experimental solubilities of benzene in aqueous $(NH_4)_2SO_4$ and NaCl solutions as a function of electrolyte concentration (in g salt/kg H_2O) at 25 °C. The symbols denote the data of Mackay and Shiu [26] and Xie et al. [27] ($(NH_4)_2SO_4$), and Shaw [28] (NaCl).

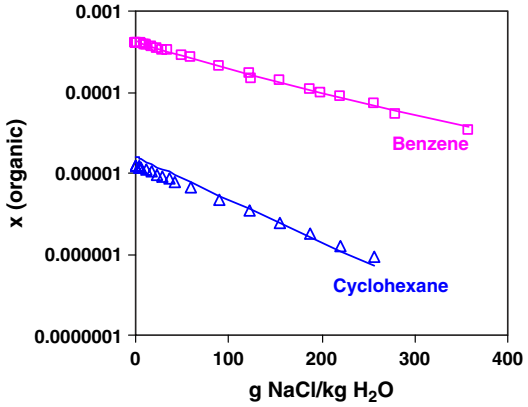

Fig. 4. Calculated and experimental solubilities of benzene and cyclohexane in aqueous NaCl solutions as a function of NaCl concentration (in g salt/kg H_2O) at 25 °C. The symbols denote the data of Shaw [28] (benzene) and Xie et al. [27] (cyclohexane).

thermodynamic properties, but fails to reproduce speciation results. The results obtained using this approach are shown in Figs. 6(a) and 7(a) for total vapor pressure and species distribution, respectively. In these figures, the properties are plotted as functions of the mole fraction of SO_3, i.e., by regarding the system as a binary mixture of SO_3 and H_2O, in which the H_2SO_4+H_2O subsystem falls in the region of $x(SO_3)$ ranging from 0 to 0.5.

In the second approach, we explicitly recognize the well-known fact that the protons that result from the dissociation of acids do not remain free in the solution but become solvated. Accordingly, protons in aqueous systems form hydronium ions (H_3O^+) with water molecules, i.e.,

$$H^+ + H_2O = H_3O^+. \quad (16)$$

To take the formation of hydronium ions into account, the dissociation reactions for sulfuric acid are rewritten as

$$H_2SO_4^0 + H_2O = HSO_4^- + H_3O^+ \quad (17)$$

$$HSO_4^- + H_2O = SO_4^{-2} + H_3O^+ \quad (18)$$

At infinite dilution in water, the standard-state properties of the hydronium ion are additive with respect to its two

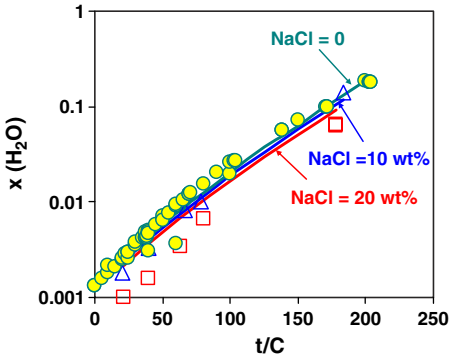

Fig. 5. Calculated and experimental solubilities of water in benzene as a function of temperature at the NaCl concentrations of 0%, 10%, and 20% (wt). The symbols denote the data of Shaw [28].

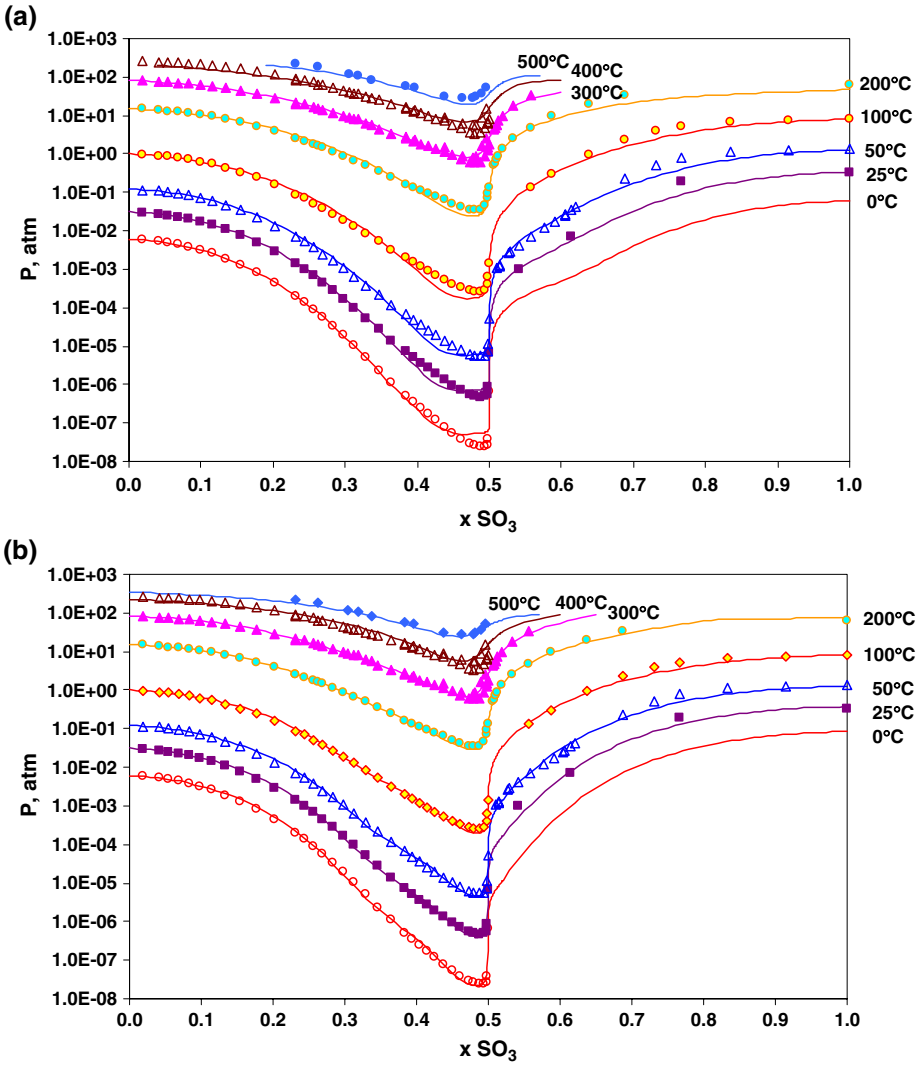

Fig. 6. Calculated and experimental vapor–liquid equilibria in the sulfuric acid/oleum system as a function of the mole fraction of SO_3 at various temperatures from 0 to 500 °C. The results are obtained using (a) the H^+ ion approach and (b) the H_3O^+ ion approach (see text). Literature data are taken from Gmitro and Vermeulen [29], Brand and Rutherford [30], Schrage [31], and Giazitzoglou and Wuster [32].

constituent entities, i.e., H^+ and H_2O. It should be noted that the hydronium ion-based approach is fully equivalent to the classical hydrogen ion-based approach in the infinite dilution limit. At this limit, a hydrogen ion embedded in an environment of n water molecules (where n is a large number) is necessarily equivalent to a combined H^++H_2O entity in an environment of $n-1$ water molecules. However, substantial differences are expected at higher concentrations because the existence of an H_3O^+ entity affects chemical equilibria and mass balance constraints, especially in water-depleted regions.

Vapor–liquid equilibrium calculations using the H_3O^+ approach are shown in Fig. 6(b) and the corresponding speciation results are given in Fig. 7(b). Experimental speciation data are available only for the H_2SO_4+H_2O system. Thus, the curves predicted for concentrations beyond pure H_2SO_4 (i.e., for $x(SO_3)>0.5$) cannot be compared with experimental data. It can be seen from Fig. 6(b) that the hydronium ion approach results in some improvement in vapor–liquid equilibrium calculations, which are now in fully quantitative agreement with experimental data under all conditions. A much more dramatic improvement is obtained for speciation as shown in Fig. 7(b). It should be noted here that the model parameters have been regressed using only thermodynamic (VLE and caloric) data and were not adjusted to match speciation data. Thus, Fig. 7(b) represents a pure prediction obtained from the model. This indicates that the hydronium ion approach puts thermodynamic modeling of acids on a much firmer basis.

5. Conclusions

A recently developed mixed-solvent electrolyte model has been applied to calculate vapor–liquid and liquid–liquid equilibria in complex water+organic+salt mixtures. The model accurately represents the effect of salts on both VLE and LLE. Also, the model has been shown to be

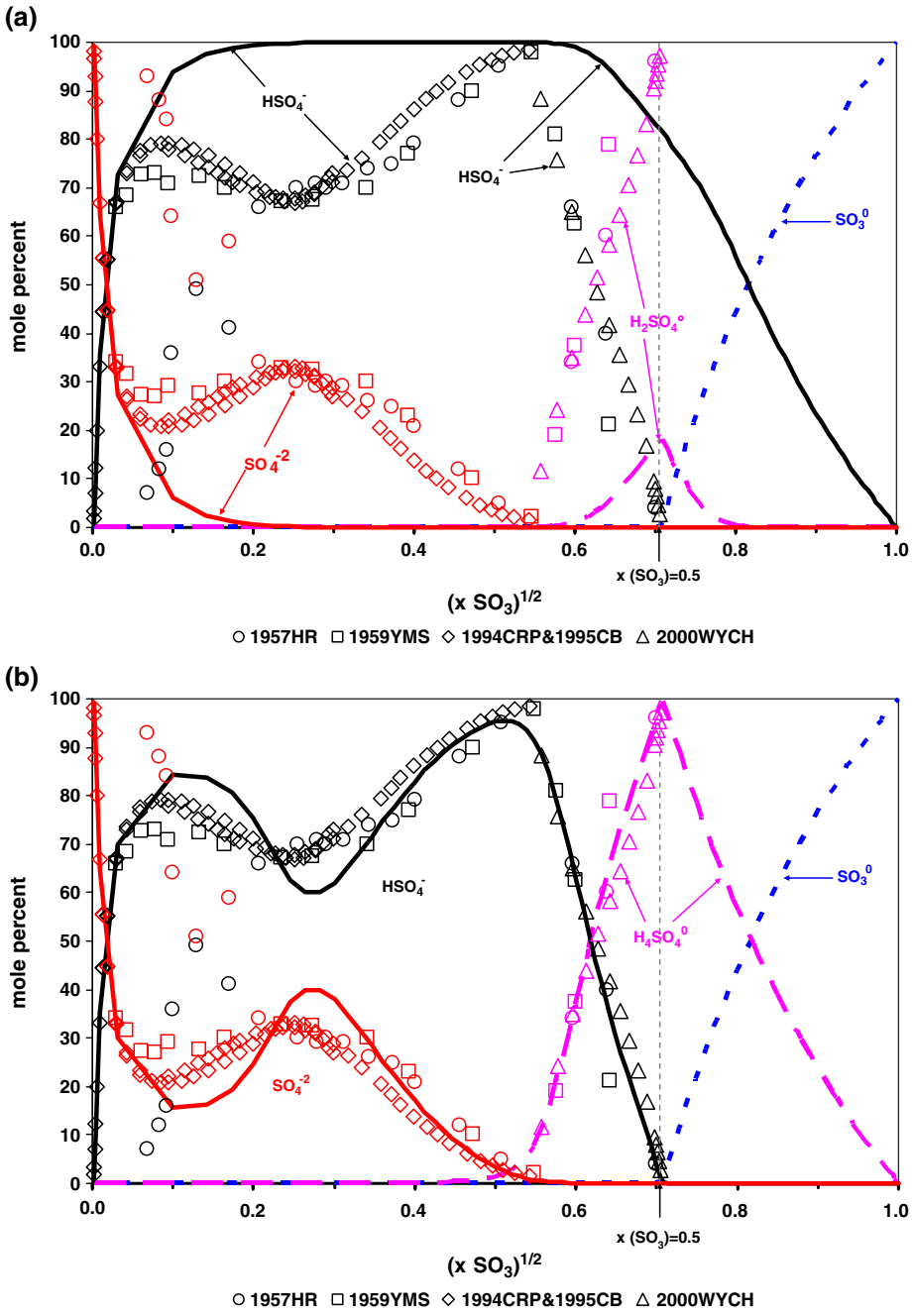

Fig. 7. Comparison of experimental and calculated species distribution in the sulfuric acid/oleum system at 25 °C. The results are obtained using (a) the H^+ ion approach and (b) the H_3O^+ ion approach (see text). Literature data are taken from Hood and Reilly [33], Young et al. [34], Walrafen et al. [35], Clegg et al. [36], and Clegg and Brimblecombe [37]. The concentration axis is given as the square root of $x(SO_3)$ to emphasize the lower concentration region.

accurate for strongly associating systems such as sulfuric acid/oleum in the entire concentration range. In addition to reproducing phase equilibria and caloric properties, the model predicts speciation that is consistent with spectroscopic measurements.

Acknowledgments

The work reported here was supported by Alcoa, Chevron, DuPont, Mitsubishi Chemical, Rohm and Haas and Shell.

Appendix A. Extension of the model to temperatures from 300 to 500 °C

The mixed-solvent electrolyte model is based on a combination of an excess Gibbs energy model (Eq. (1)) and the Helgeson–Kirkham–Flowers (HKF) [7–11] equation for standard-state properties. In general, models that are based on an explicit formulation for the excess Gibbs energy of the liquid phase are limited to temperatures that are reasonably lower than the critical temperature of the system. As a rule of thumb, such models can be used at temperatures that do not

exceed roughly $0.9T_c$, where T_c is the critical temperature of a mixture. Thus, the model can be applied to dilute aqueous system at temperatures up to ca. 300 °C. However, the upper temperature limit of the model can be extended for concentrated electrolyte solutions, whose critical temperature is typically much higher than the critical temperature of water. The $H_2SO_4–H_2O–SO_3$ system is an example of such a solution. For such systems, the model is expected to be applicable only in the concentrated solution range and will unavoidably break down for dilute solutions.

Although the excess Gibbs energy model can be directly applied to such high-temperature systems (provided that they are subcritical), there is a need for modifying the standard-state property model. This is due to the fact that the standard-state property model is defined at infinite dilution in water and, hence, is strongly affected by the temperature and pressure variations of pure water properties in the near-critical region of water. At the same time, the effect of near-critical variations in water properties is gradually attenuated with rising electrolyte concentration and effectively vanishes for highly concentrated solutions. Therefore, there is a need to use effective standard-state properties of individual species that are not affected by the near-critical behavior of water and, therefore, are applicable to model concentrated solutions at temperatures above ca. 300 °C. In this study, we define the effective standard-state properties for simulating high-temperature concentrated solutions in the following way:

(1) At temperatures below 300 °C, the standard-state properties are calculated directly from the Helgeson–Kirkham–Flowers EOS for both dilute and concentrated solutions.
(2) At temperatures above 300 °C, we assume constant (i.e., temperature- and pressure-independent) standard-state heat capacities and volumes, which are obtained at $t=300$ °C. The standard Gibbs energy, enthalpy and entropy are then calculated by thermodynamic integration using the heat capacity and volume at 300 °C. This eliminates the near-critical effects that result from water properties and makes the model applicable to high-temperature (up to 500 °C) mixtures, provided that they are substantially subcritical.

References

[1] P. Wang, A. Anderko, R.D. Young, Fluid Phase Equilib. 203 (2002) 141.
[2] P. Wang, R.D. Springer, A. Anderko, R.D. Young, Fluid Phase Equilib. 222–223 (2004) 11.
[3] K.S. Pitzer, J. Phys. Chem. 77 (1973) 268.
[4] K.S. Pitzer, J. Am. Chem. Soc. 102 (1980) 2902.
[5] P. Wang, A. Anderko, Fluid Phase Equilib. 186 (2001) 103.
[6] D.S. Abrams, J.M. Prausnitz, AIChE J. 21 (1975) 116.
[7] H.C. Helgeson, D.H. Kirkham, G.C. Flowers, Am. J. Sci. 274 (1974) 1089;
ibid. 274 (1974) 1199;
ibid. 276 (1976) 97;
ibid. 281 (1981) 1241.
[8] E.L. Shock, H.C. Helgeson, D.A. Sverjensky, Geochim. Cosmochim. Acta 53 (1989) 2157.
[9] E.L. Shock, H.C. Helgeson, Geochim. Cosmochim. Acta 52 (1988) 2009; ibid. 54 (1990) 915.
[10] E.L. Shock, D.C. Sassani, M. Willis, D.A. Sverjensky, Geochim. Cosmochim. Acta 61 (1997) 907.
[11] D.A. Sverjensky, E.L. Shock, H.C. Helgeson, Geochim. Cosmochim. Acta 61 (1997) 1359.
[12] J.Y. Zuo, D. Zhang, W. Fürst, AIChE J. 46 (2000) 2318.
[13] H. Zerres, J.M. Prausnitz, AIChE J. 40 (1994) 676.
[14] Y. Liu, S. Watanasiri, Fluid Phase Equilib. 116 (1996) 193.
[15] L.R. Pratt, J. Phys. Chem. 96 (1992) 25.
[16] C.A. Haynes, H.W. Blanch, J.M. Prausnitz, Fluid Phase Equilib. 53 (1989) 63.
[17] C.A. Haynes, J. Carson, H.W. Blanch, J.M. Prausnitz, AIChE J. 37 (1991) 1401.
[18] T.F. Anderson, J.M. Prausnitz, Ind. Eng. Chem. Process Des. Dev. 17 (1978) 561.
[19] R.C. Reid, J.M. Prausnitz, B.E. Poling, The Properties of Gases and Liquids, 4th ed., McGraw-Hill Book Company, New York, 1987.
[20] H. Brusset, J. Gaynes, C.R. Acad. Sci. 236 (1953) 1563.
[21] A.N. Campbell, J. Am. Chem. Soc. 67 (1945) 981.
[22] A.N. Campbell, J.R. Campbell, J. Am. Chem. Soc. 59 (1937) 2481.
[23] C.F. Prutton, T.J. Walsh, A.M. Desai, Ind. Eng. Chem. 42 (1950) 1210.
[24] R.V. Lyzlova, M.P. Susarev, Zh. Prikl. Khim. (Leningrad) 55 (1982) 261.
[25] F.A.H. Schreinemakers, Z. Phys. Chem. 39 (1902) 485.
[26] D. Mackay, W.-Y. Shiu, Can. J. Chem. Eng. 53 (1975) 239.
[27] W.-H. Xie, W.-Y. Shiu, D. Mackay, Mar. Environ. Res. 44 (1997) 429.
[28] D. Shaw, Solubility Data Series: Part 1. Hydrocarbons C_5 to C_7, vol. 37, Pergamon Press, NewYork, 1989.
[29] J.I. Gmitro, T. Vermeulen, AIChE J. 10 (1964) 740.
[30] J.C.D. Brand, A. Rutherford, J. Chem. Soc. (1952) 3916.
[31] J. Schrage, Fluid Phase Equilib. 68 (1991) 229.
[32] Z. Giazitzoglou, G. Wuster, in: Berichte der Bunsen Gesellschaft fuer Physikalische Chemie, vol. 85, 1981, p. 127.
[33] G.C. Hood, C.A. Reilly, J. Chem. Phys. 27 (1957) 1126.
[34] T.F. Young, L.F. Maranville, H.M. Smith, The Structure of Electrolyte Solutions, 1959, p. 35.
[35] G.E. Walrafen, W.-H. Yang, Y.C. Chu, M.S. Hokmabadi, J. Solution Chem. 29 (2000) 905.
[36] S.L. Clegg, J.A. Rard, K.S. Pitzer, J. Chem. Soc., Faraday Trans. 90 (1994) 1875.
[37] S.L. Clegg, P. Brimblecombe, J. Chem. Eng. Data 40 (1995) 43.